

CAAP Quarterly Report

Date of Report: *Nov 30, 2020*

Prepared for: *U.S. DOT Pipeline and Hazardous Materials Safety Administration*

Contract Number: 693JK320NF0001

Project Title: *Holistic Electromagnetic and Ultrasonic NDE Techniques for Plastic Pipeline Aging and Degradation Characterization*

Prepared by: *Subrata Mukherjee (PhD student), Xiaodong Shi (PhD student), Dr. Jiaoyang Li (Postdoc fellow), Dr. Yiming Deng (PI)*

Contact Information: *Dr. Yiming Deng (MSU), Dr. Yongming Liu (ASU), Dr. Sunil Chakrapani (MSU), Dr. Changyong Cao (MSU)*

For quarterly period ending: *Nov 30, 2020*

Business and Activity Section

(a) Contract Activity

Nothing to report.

(b) Status Update of Past Quarter Activities

The kick-off meeting was held on Nov. 30th.

(c) Cost share activity

Nothing to report.

(d) Task 1: Near field microwave based flexible electromagnetic transducer

1. Background and Objectives

Test methods based on the microwave are increasingly becoming famous for characterizing non conducting materials and detecting and imaging defects in non-destructive applications because of contactless inspection. Due to the increasing availability of low-cost integrated microwave components, microwave testing has gathered immense attention in the NDE community. Microwaves are basically those electromagnetic waves covering the wavelength range from decimeter down to the millimeter, corresponding to frequencies ranging from 0.3 GHz to 300 GHz. These waves can penetrate electrically nonconductive materials; hence, they are used in NDT of pipelines, ceramics, concretes, polymeric materials, and fiber composites [1]. This quarter, we have done a literature review of the various types of split-ring resonators (SRRs) and their effectiveness in detecting various types of NDE detections in composites and detecting plasticity loss in pipelines. The super-resolution capability to detect even the subsurface

defects, high Q factor, low insertion loss is some of the reasons why SRR sensors are effective in NDE inspections and thus provides an interesting platform for assessing structural integrity and reliability. Major advantages of microwave NDE inspections are as follows:

- Microwaves can propagate through materials without suffering much attenuation [2].
- Single-sided access non-contact nature are some other benefits and thus provide rapid inspections.

The introduction of the initial SRR structure is inspired by Pendry's pioneering works in 1999 [3]. Since then, SRR has been a hot topic in the metamaterials research fraternity [4,5]. The left-handedness was first visioned by the Russian physicist Victor Veselago in [6]. The LH material was not a natural substance but an artificial, effectively homogeneous substance [7]. To possess a negative refractive index, both the parameters ϵ and μ have to be negative. As there exists not a substance with both ϵ and μ negative, but it is observed two different substances with each one having one of the constituent parameters as negative can be coupled together, which behaves as an LH medium. The plasma-like behavior is responsible for negative dielectric permittivity at a frequency less than plasma frequency [8,9]. SRRs follow this working principle, and thus the design constitutes conducting wire loops with a split that behaves like magnetic plasma [10].

2. Working Principle and Designs of different SRRs:

SRR consists of two concentric metallic rings separated by a gap and having both splits at opposite ends, as shown in figure 1. Due to the splits (s) at the rings and the gap (g) between the inner and outer rings, magnetic resonance is induced. The plasmonic type negative permeability function is exhibited when the excitation magnetic field is perpendicular to the magnetic field's plane. SRRs are basically sub-wavelength resonators when excited by a time-varying magnetic field perpendicular to the rings' plane. They hence can propagate signals in a narrow band close to their resonant frequency [11]. SRRs behave as parallel LC resonating structures [12]. The induced resonating current flows along with the rings with charges preventing the current from flowing around the ring, thus completing the circuit across the two rings' small capacitive gaps. The resonant frequency achieved here depends on the unit cell parameters like ring size, width, and edge gaps. It is excited by the microstrip line's H-filed rather than directly connected and steals energies from the microstrip line at resonant frequencies. Thus, these structures are widely used in bio-sensing applications [13]. It possesses a band-stop structure that allows the integration of multiple cells on the microstrip line, resonating at different frequencies.

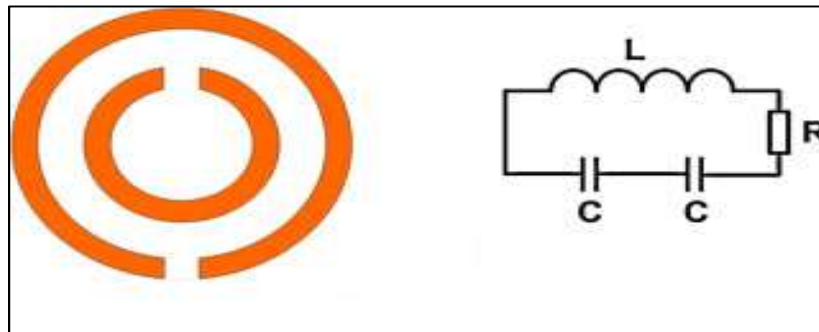


Figure 1: Split ring resonator and its equivalent circuit

Parameters influencing the magnetic resonance:

A: Capacitance & Inductance in SRR

A SRR unit cell behaves as a LC circuit where the resonant frequency (f) is given by $f = 1/2\pi\sqrt{LC}$ Where L and C are the effective inductance and capacitance of each cell, the inductance is basically due to the inductance and coupling between two rings. The capacitance is due to the split gap of each ring and mutual capacitance between the rings. Split contributes to the capacitance and is also responsible for the negative permeability of the structure. The outer ring is oriented in the opposite direction to the inner, and it lowers the resonant frequency by generating a large capacitance across the gaps between the rings. Thus, these structures behave as narrowband suppression, high Q resonators. Figure 2 shows the topology of the SRR sample behaving as a sensor.

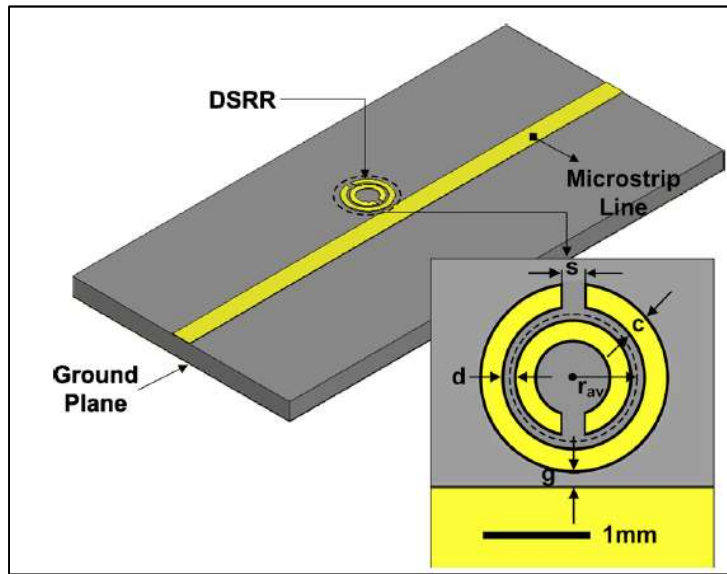


Figure 2: SRR sensor along with microstrip line

B: Effect of different physical dimensions on resonant frequency:

Different physical dimensions of SRR are varied, which affect the capacitance, thereby changing the resonant frequency. The effect of split width, gap distance, metal width, and additional capacitance is as follows:

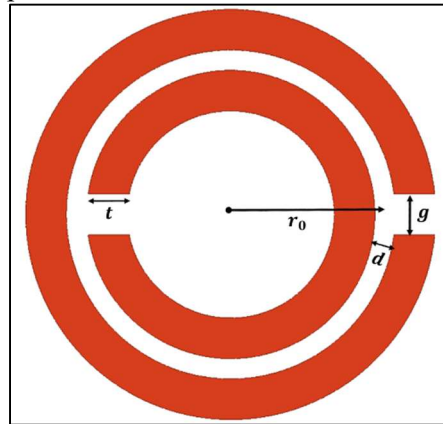


Figure 3: SRR Unit cell different governing parameters

- I. Effect of ring radius: Increasing the ring radius r_0 means increase in metallic surface area and thereby increase in ring inductance as well as capacitance. Now increase in L and C means decrease in resonant frequency and hence the increase in Q factor which is desired as $Q^{-1} = \delta / r_0$ where δ is the skin depth. Thus, the sensitivity increases at the cost of size of the sensor. Hence the ring radius has to be optimized.
- II. Effect of split thickness (t): Increase in thickness of the ring increases the ring inductance because of the increase in surface current and also the capacitance due to the increase in surface area. Thus the resonant frequency decrease and hence Q factor and sensitivity increases.
- III. Effect of split gap (g): As the gap increases the resonant frequency increases due to the decrease in inductance and capacitance, thereby causing decrease in Q factor. Hence though the penetration increases but the resolution decreases.
- IV. Effect of ring separation (d): An increase in ring separation has counterbalancing effect as the mutual capacitance and inner ring inductance decreases but with the increase in outer ring inductance.

- V. Effect of additional capacitance: On increasing capacitance by adding capacitors to the outer ring in parallel, the capacitance increases thereby decreasing the resonant frequency.

These parameters are thereby optimized to achieve the minimum insertion loss and high Q factor. Now, more weightage is on reducing the insertion loss than on the Q factor. Hence in Ansys, the following parameters give rise to the minimum insertion loss.

Different designs and types of SRR: The efficient design of the SRRs has two splits placed symmetrically opposite to each other. Electric dipole moments cancel out each other and thus decrease the effect of electric polarizability. SRR is generally bianisotropic i.e., an electric dipole moment develops across the capacitive gaps. The below figure shows the schematic of the different unit cells of SRR containing various rings and splits, thereby altering the resonant frequency [14].

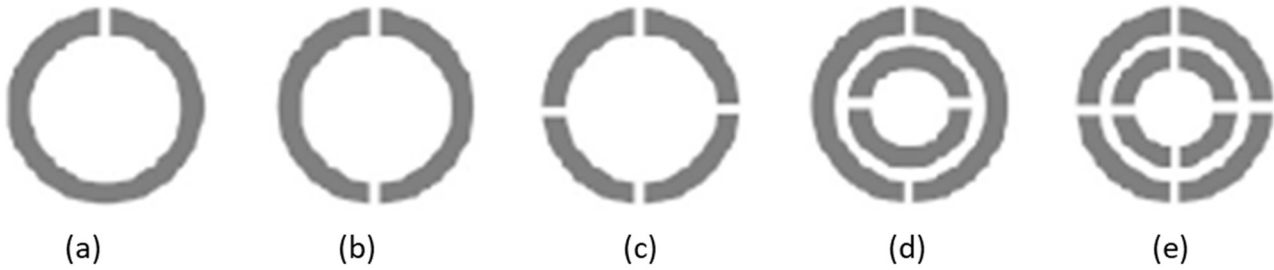


Figure 4: Variations in rings and gaps in single cell of SRR

Complementary SRR (CSRR) is another type of SRR which was first introduced in [15] where CSRRs were etched in the ground plane of a microstrip line of impedance 50 ohm and it was stated that due to Babinet principle and complementarity, the CSRR loaded line should behave as a one-dimensional effective medium with a negative value of the dielectric permittivity in a narrow band in the vicinity of CSRR resonance. In an equivalent model of CSRR like that of SRR, the series connection of the capacitances is substituted by the parallel combination of the inductances as shown in below figure. However, in SRR based sensors the degree of freedom is more than that in CSRR sensors [16].

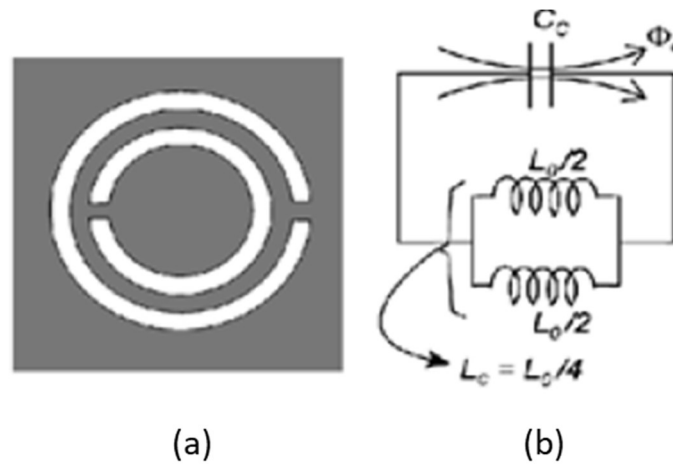


Figure 5: Basic schematic of CSRR

Defect detection using rigid SRR sensor: In our lab, we have fabricated rigid SRR sensors, as shown in figure 6. Samples are scanned from the edge of the sensor for effective scanning. One SRR ring is used to sense, whereas the other ring, called the reference ring, is placed on the other side of the microstrip line. During the entire scanning process, the reference ring's resonant frequency does not change as it never interacts with the sample. In contrast, the sensing ring changes the resonant frequency as it is in close vicinity to the sample. Hence it will be much more efficient to observe the sensing ring's frequency shift concerning the reference ring.

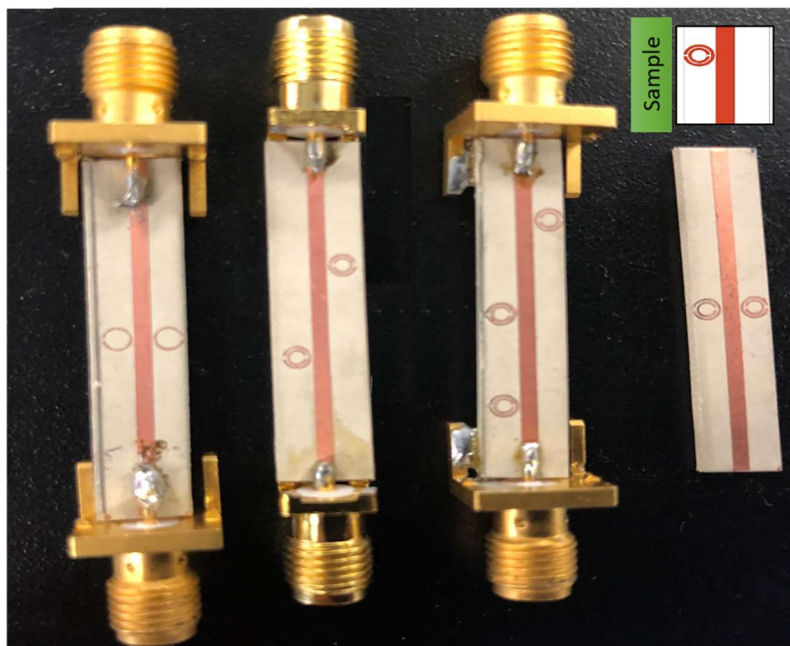
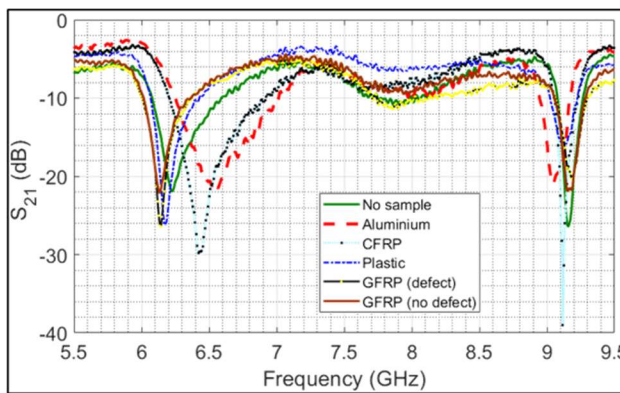
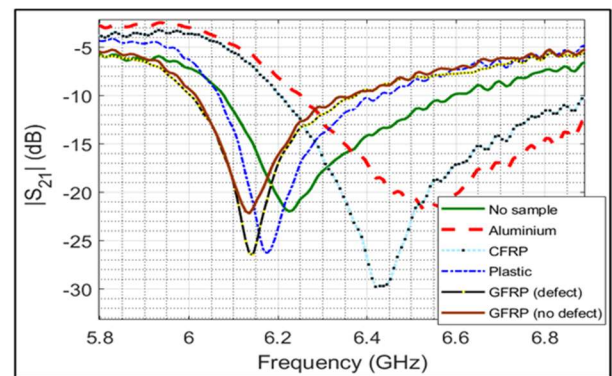


Figure 6: Fabrication of rigid SRR containing sensing and reference SRRs.

The sensor's insertion loss is then measured using an E5070B Vector Network Analyzer (VNA). Two resonant peaks are observed due to sensing and reference ring. Figure 7 (a) the first resonance corresponds to the sensing ring, whereas the second resonance is due to the reference SRR. Due to the change in the dielectric property, the resonant frequency of the sensing SRR changes in the presence of materials, whereas the reference SRR remains the same. The resonant frequency shifts to the right to conductive materials like Aluminium, CFRP, etc., whereas it shifts to the left in the presence of dielectric materials like plastic, GFRP. This shows that the sensor is sensitive to dielectric and conductive changes in the sample, as evident in figure 7 (b).



(a)



(b)

Figure 7: (a) Insertion loss in the sensor, (b) Frequency shift in sensing ring due to change in dielectric property in presence of sample

Figure 8 shows that we are successful in imaging and detecting various surface and surface defects with high accuracy in an additive manufacturing sample. The sample's dimension is $35\text{ mm} \times 50\text{ mm} \times 8\text{ mm}$. The sub-mm defects on the side can also be detected.

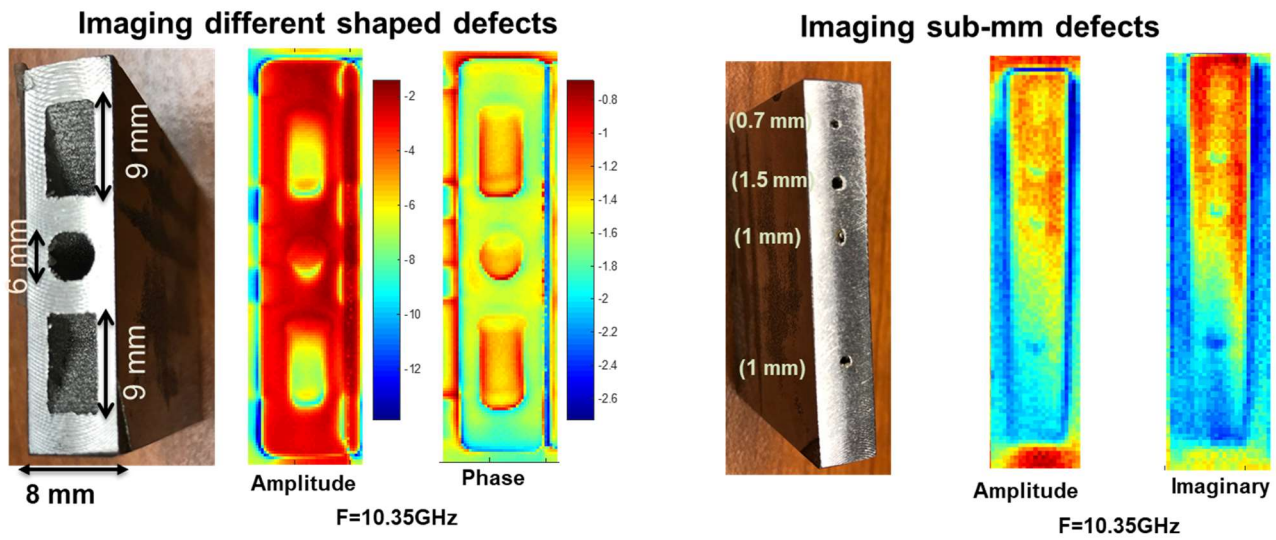


Figure 8: Imaging surface and subsurface defects by the rigid sensor

Need for Flex SRR sensors: When the Material under test (MUT) possess complex structures which are basically curved like in pipelines there to detect defects by rigid sensors give rise to errors as these SRR structures do not fit the sample and thus different areas will be at different lift off from the sensor.

Flex sensors are very effective as they conform to the sample's shape, and thus every part of the MUT will be at the same lift-off from the sensor. Figure 9 shows the problem of scanning with a rigid sensor and the efficacy of using flex sensors while sensing on an Al Circular arc-shaped sample containing a small defect of radius 2 mm. Initial studies in [17, 18, 19] have inspired us to designed and fabricate flex sensors where the benefits are as follows:

- Ease of integration to complicated shapes and thus possessing a constant lift-off to MUT
- Light weight, compact and cheap to manufacture
- Conforms to different specimen and thus can be easily embedded in the structures

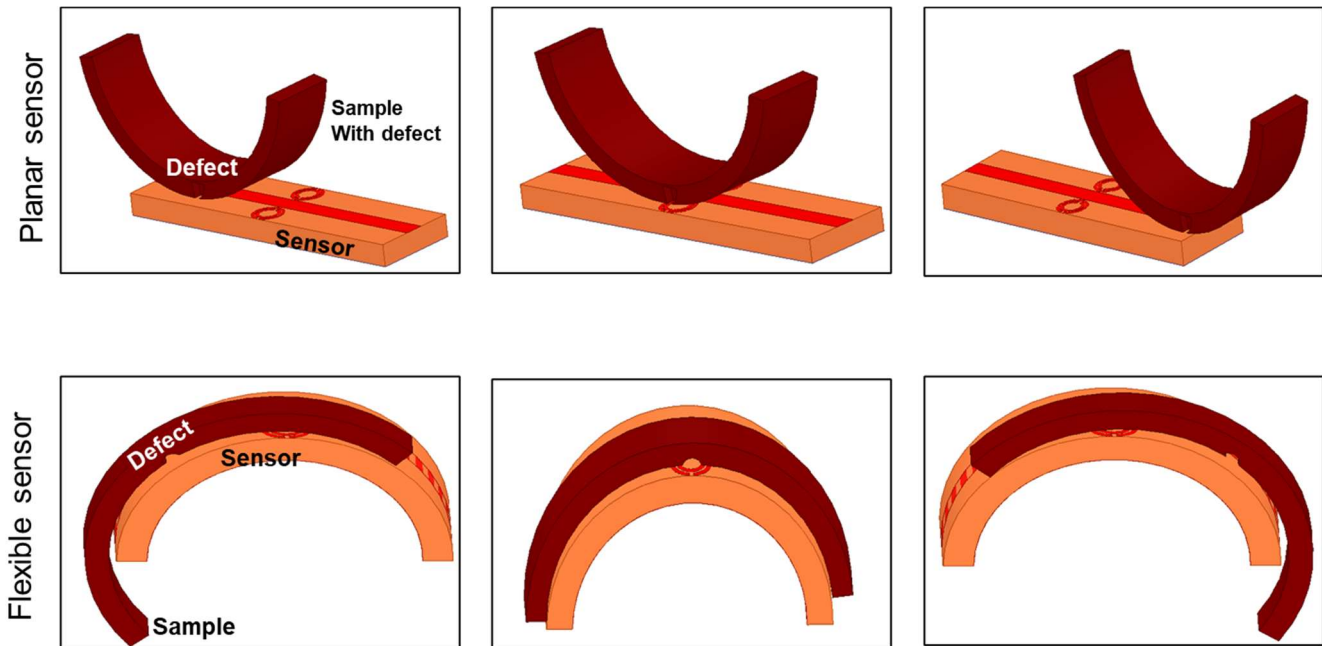


Figure 9: (a) Planar sensor do not conform to the shape of MUT, (b) Flex sensor conforming to the shape of MUT and thus a constant liftoff

3. Simulation & Experimental Results for flex SRR sensor:

Using ANSYS HFSS, the Flex SRR sensor's electromagnetic model has been developed. We have then studied whether the insertion loss is affected by variations in dielectric properties due to the usage of various substrates and different curvatures. A microstrip line of impedance 50 ohm and length 20 mm, and thickness 0.125 mm has been chosen for this purpose.

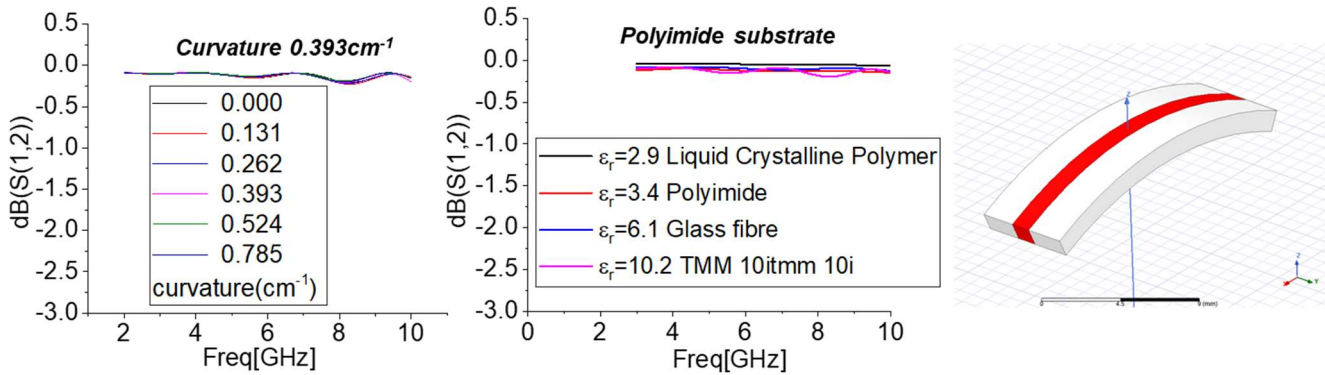


Figure 10: Effect on insertion loss by variations of dielectric properties and curvature

Figure 10 shows that insertion loss is unaffected by variations in dielectric properties and curvature.

Two configurations are presented where the MUT is first placed parallel to the sensing ring and then on the sensing ring's top. Figure 11 (a) and (b) show that the insertion losses are more prominent when the sample under test is placed on the top of the sensor rather than on the side. Figure 11 (c) shows the shift in resonant frequency due to loading from different samples at different flex sensors' curvatures. From 11 (c), we can conclude that the resonant frequency increases for conductive samples, and it decreases for dielectric samples.

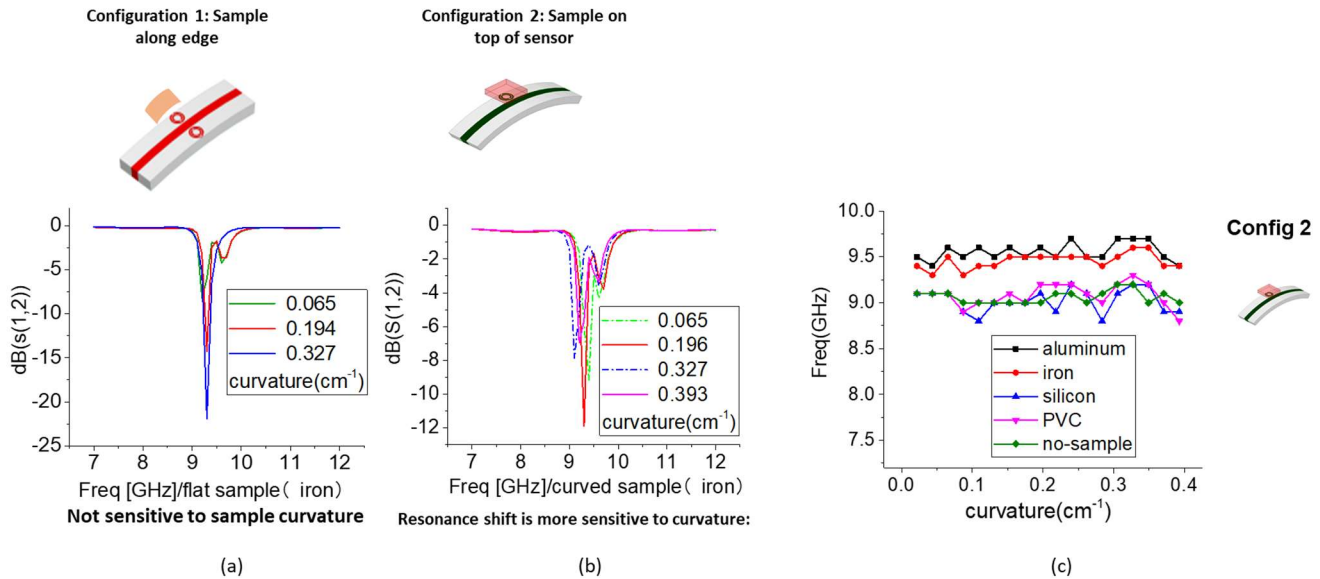


Figure 11: (a) Sample placed along the edge of the sensing sensor (b) Sample placed on the top of the sensor, (c) Insertion loss for different sample materials at different radius of curvature of the flex sensor.

Now in simulation we have shown how the resonance shifts correlates more accurately to defect size on using flexible sensors when compared to that with rigid sensor. Figure 12 (a) and (b) compares the amplitude and phase response of insertion loss vs the scanning distance on using rigid and flex sensors. From the below figure it is clearly seen that the resonance shifts correlate more closely to the defect size for flex sensors.

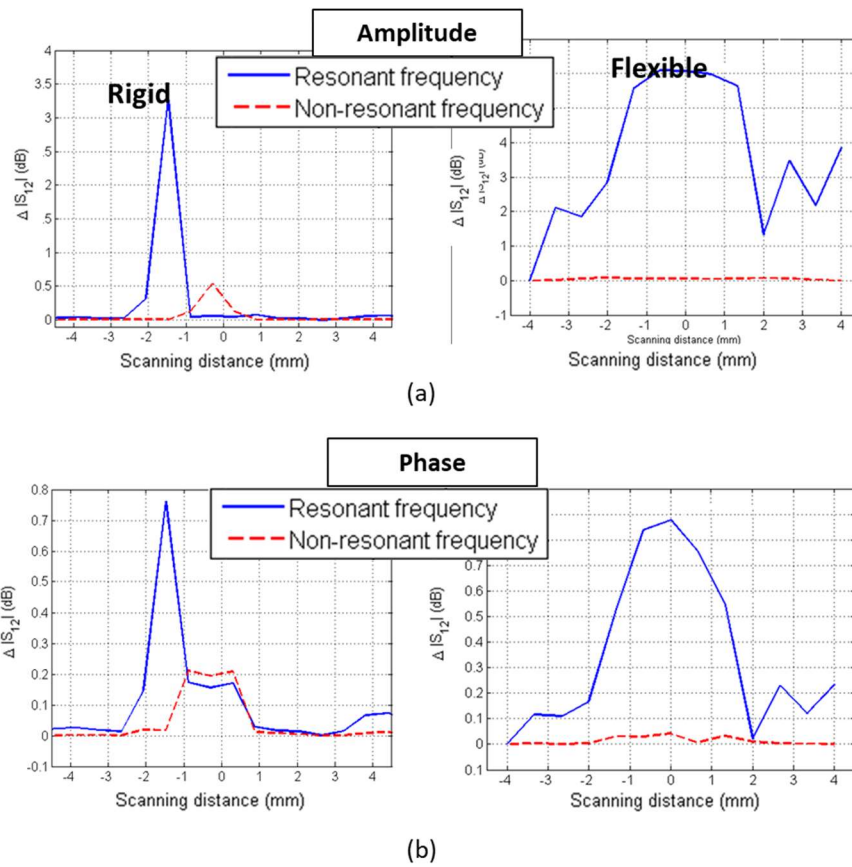


Figure 12: amplitude and phase response of insertion loss for rigid and flex sensors

Next, in order to validate the results experimentally, we need to fabricate the flex sensors. We have built a preliminary Flexible sensor that can conform to the complex geometry shapes of the samples. However, a more robust sensor needs to be fabricated in the following quarters to detect the plasticity loss in pipelines such that the sensor is not fragile. An initial Flex sensor was fabricated using Aerosol jet printing and E beam thermal decomposition. Here Kapton Polyimide film of $50 \mu\text{m}$ thickness was used as the substrate of the flexible sensor. The SRR and microstrip lines are printed with Ag nanoparticle ink, while the ground plane is made up of Al film of $1.5 \mu\text{m}$ thickness. Figure 13 (a) shows a fabricated printed circuit board, (b) shows a flexible sensor integrated with electrical connections, (c) shows a resonant response due to the SRR ring, which abides by the fabrication process. The fabrication of the sensor will be carried out in the next quarter.

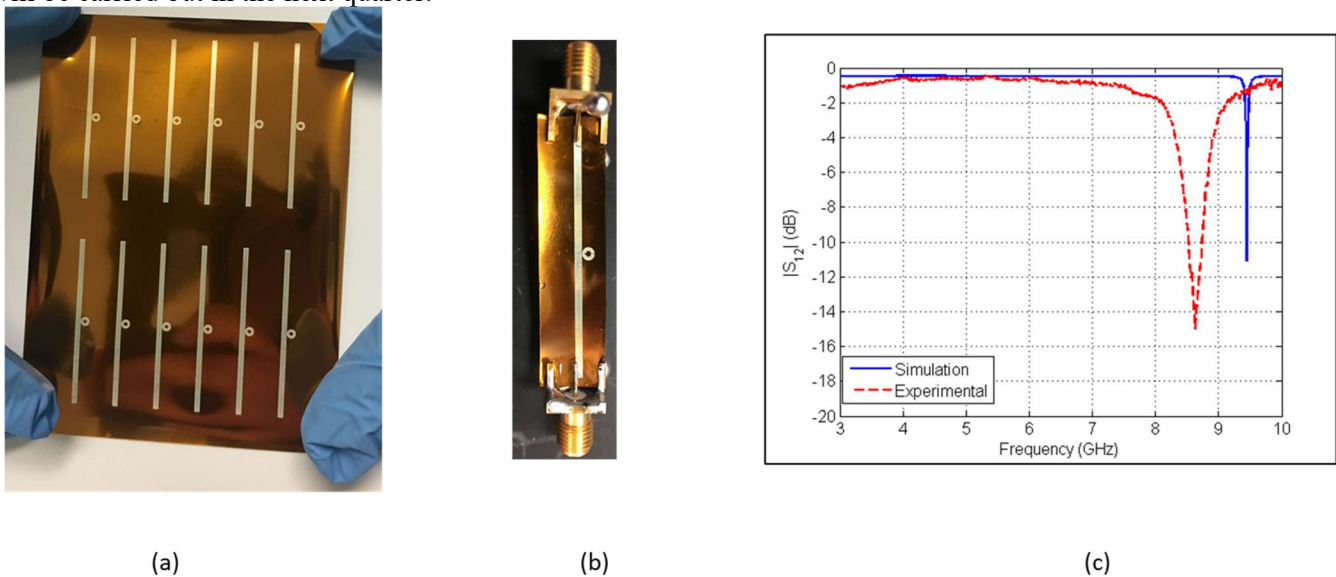


Figure 13: (a) showing fabricated printed circuit board, (b) flex sensor with connections, (c) simulated and experimental resonant frequency for SRR flex sensor.

4. Future work

In this quarter, literature reviews of the flexible sensors and near-field microwave methods have been done. Some simulation studies that analyze the performance of the Flex-SRR have been performed. As discussed above, flex SRR sensors can detect the defects from MUT's complex geometries; hence, in the next quarter, we will fabricate flex sensors and use them to detect plasticizer loss in pipelines. Plasticizer is an additive added to another material (usually plastic or elastomer) to make that material softer and more pliable. As the pipelines in practice wear away due to usage, plasticizer loss is a common phenomenon in the pipeline industry, and there is a need to address these losses accurately. These losses, which occur gradually due to diffusion and evaporation over time uniformly within the pipeline, are hard to detect by conventional NDE methods. As the flex sensors are well sensitive to dielectric changes in complex geometries, we will address the efficacy of flex-SRR sensors in detecting plasticizer losses in working pipelines in the next quarter.

References

- [1] Zoughi, Reza, and Sergey Kharkovsky. "Microwave and millimetre wave sensors for crack detection." *Fatigue & Fracture of Engineering Materials & Structures* 31, no. 8 (2008): 695-713.
- [2] Mukherjee, Saptarshi, Antonello Tamburrino, Mahmoodul Haq, Satish Udpa, and Lalita Udpa. "Far field microwave NDE of composite structures using time reversal mirror." *NDT & E International* 93 (2018): 7-17.
- [3] Pendry, John B., Anthony J. Holden, David J. Robbins, and W. J. Stewart. "Magnetism from conductors and enhanced nonlinear phenomena." *IEEE transactions on microwave theory and techniques* 47, no. 11 (1999): 2075-2084.
- [4] Withayachumnankul, Withawat, Kata Jaruwongrungrsee, Adisorn Tuantranont, Christophe Fumeaux, and Derek Abbott. "Metamaterial-based microfluidic sensor for dielectric characterization." *Sensors and Actuators A: Physical* 189 (2013): 233-237.
- [5] Labidi, Mondher, Jamel Belhadj Tahar, and Fethi Choubani. "Meta-materials applications in thin-film sensing and sensing liquids properties." *Optics express* 19, no. 104 (2011): A733-A739.
- [6] Iyer, Ashwin K., and George V. Eleftheriades. "Negative refractive index metamaterials supporting 2-D waves." In *2002 IEEE MTT-S International Microwave Symposium Digest (Cat. No. 02CH37278)*, vol. 2, pp. 1067-1070. IEEE, 2002.
- [7] Iyer, Ashwin K., and George V. Eleftheriades. "Negative refractive index metamaterials supporting 2-D waves." In *2002 IEEE MTT-S International Microwave Symposium Digest (Cat. No. 02CH37278)*, vol. 2, pp. 1067-1070. IEEE, 2002.
- [8] Pendry, John B., A. J. Holden, W. J. Stewart, and I. Youngs. "Extremely low frequency plasmons in metallic mesostructures." *Physical review letters* 76, no. 25 (1996): 4773.
- [9] Pendry, John B., A. J. Holden, W. J. Stewart, and I. Youngs. "Extremely low frequency plasmons in metallic mesostructures." *Physical review letters* 76, no. 25 (1996): 4773.
- [10] Aydin, Koray, Irfan Bulu, Kaan Guven, Maria Kafesaki, Costas M. Soukoulis, and Ekmel Ozbay. "Investigation of magnetic resonances for different split-ring resonator parameters and designs." *New journal of physics* 7, no. 1 (2005): 168.
- [11] Isakov, Dmitry, Chris J. Stevens, Flynn Castles, and Patrick S. Grant. "A split ring resonator dielectric probe for near-field dielectric imaging." *Scientific reports* 7, no. 1 (2017): 1-9.
- [12] Baena, Juan Domingo, Jordi Bonache, Ferran Martín, R. Marqués Sillero, Francisco Falcone, Txema Lopetegui, Miguel AG Laso et al. "Equivalent-circuit models for split-ring resonators and complementary split-ring resonators coupled to planar transmission lines." *IEEE transactions on microwave theory and techniques* 53, no. 4 (2005): 1451-1461.

- [13] Lee, Hee-Jo, and Jong-Gwan Yook. "Biosensing using split-ring resonators at microwave regime." *Applied Physics Letters* 92, no. 25 (2008): 254103.
- [14] Reddy, A. Nutan, and S. Raghavan. "Split ring resonator and its evolved structures over the past decade: This paper discusses the nuances of the most celebrated composite particle (split-ring resonator) with which novel artificial structured materials (called metamaterials) are built." In *2013 IEEE International Conference ON Emerging Trends in Computing, Communication and Nanotechnology (ICECCN)*, pp. 625-629. IEEE, 2013.
- [15] Falcone, Francisco, Txema Lopetegui, Juan D. Baena, Ricardo Marqués, Ferran Martín, and Mario Sorolla. "Effective negative-/spl epsiv/stopband microstrip lines based on complementary split ring resonators." *IEEE microwave and wireless components letters* 14, no. 6 (2004): 280-282.
- [16] Shafi, KT Muhammed, Abhishek Kumar Jha, and Mohammad Jaleel Akhtar. "Improved planar resonant RF sensor for retrieval of permittivity and permeability of materials." *IEEE Sensors Journal* 17, no. 17 (2017): 5479-5486.
- [17] Korostynska, O., A. Mason, and A. I. Al-Shamma'a. "Proof-of-concept microwave sensor on flexible substrate for real-time water composition analysis." In *2012 Sixth International Conference on Sensing Technology (ICST)*, pp. 547-550. IEEE, 2012.
- [18] Yang, Siming, Peng Liu, Liang Dong, and Jiming Song. "Microwave meta-skin for tunable frequency selective surface and flexible invisibility cloak." In *2016 IEEE International Symposium on Antennas and Propagation (APSURSI)*, pp. 367-368. IEEE, 2016.
- [19] Islam, Mohammad Tariqul, Touhidul Alam, Iskandar Yahya, and Mengu Cho. "Flexible radio-frequency identification (RFID) tag antenna for sensor applications." *Sensors* 18, no. 12 (2018): 4212.